Precursor Phenomena at the Magnetic Ordering of the Cubic Helimagnet FeGe

H. Wilhelm,[1] M. Baenitz,[2] M. Schmidt,[2] U. K. Rößler,[3] A. A. Leonov,[3] and A. N. Bogdanov[3]

[1]*Diamond Light Source Ltd., Chilton, Didcot, Oxfordshire, OX11 0DE, United Kingdom*

[2]*Max Planck Institute for Chemical Physics of Solids, Nöthnitzer-Str. 40, 01187 Dresden, Germany*

[3]*IFW Dresden, Postfach 270116, 01171 Dresden, Germany*

(Received 27 December 2010; revised manuscript received 7 May 2011; published 13 September 2011)

We report on detailed magnetic measurements on the cubic helimagnet FeGe in external magnetic fields and temperatures near the onset of long-range magnetic order at $T_C = 278.2(3)$ K. Precursor phenomena display a complex succession of temperature-driven crossovers and phase transitions in the vicinity of T_C. The A-phase region, present below T_C and fields $H < 0.5$ kOe, is split in several pockets. The complexity of the magnetic phase diagram is theoretically explained by the confinement of solitonic kinklike or Skyrmionic units that develop an attractive and oscillatory intersoliton coupling owing to the longitudinal inhomogeneity of the magnetization.

DOI: 10.1103/PhysRevLett.107.127203 PACS numbers: 75.30.Kz, 75.10.−b

The peculiarities of the electronic [1] and magnetic [2] properties of the monosilicides of transition metals crystallizing in the $B20$ structure (space group $P2_13$) attract unabated attention. The magnetically ordered $B20$ compounds are chiral cubic helimagnets as a consequence of the broken inversion symmetry and the Dzyaloshinskii-Moriya (DM) interaction [3,4]. The paramagnetic (PM) to helimagnetic transition in these compounds is a long-standing and unsolved problem that seems to be related to the specific frustration introduced by the chiral DM interactions. Intensive experimental investigations of the archetypical chiral helimagnet MnSi report numerous physical anomalies along the magnetic ordering transition, and particularly, indicate the existence of a small closed area in the magnetic field—temperature, (H, T), phase diagram, the so-called "A phase" [5–16]. Magnetic neutron diffraction data first suggested a paramagnetic nature of the magnetic state in the A phase [10], but later static magnetic modulations transverse to the field direction were found [14]. The attempts to explain the A phase by the formation of a specific modulated phase either with a one-dimensional modulation ("single-q" helicoids) [15–17] or as "triple-q" modulated textures [13] are in contradiction to earlier magnetization data suggesting a subdivided A phase in MnSi [9] as well as a rigorous theoretical analysis [18,19].

Theory has predicted the existence of chiral precursor states near magnetic ordering [19,20] and specific Skyrmionic textures composed of stringlike localized states [21,22]. Recent direct observations of specific two-dimensional modulations in $Fe_{0.5}Co_{0.5}Si$ [23] and FeGe [24] as well as isolated and bound chiral Skyrmions in $Fe_{0.5}Co_{0.5}Si$ [2] and FeGe [25] at low T conclusively prove the existence of Skyrmions in nanolayers of cubic helimagnets. However, the relation between the precursor phenomena in bulk material very close to T_C with the direct microscopic observations at much lower T in nanolayers [2,25] and the theoretical predictions of stable $-\pi$ Skyrmions [21,22] is still an open question [18].

In this Letter we present ac-susceptibility data on the cubic modification of FeGe, ϵ-FeGe, close to the onset of magnetic order. FeGe is an important counterpart to MnSi as a cubic helimagnet, because it behaves magnetically differently [26–28]. Spin fluctuations are less relevant than in MnSi as the Fe ions bear a stable magnetic moment characteristic for strong band-ferromagnets [29]. Our results conclusively show that the A-phase region is not a distinct simple phase. The succession of crossovers and phase transitions can be interpreted as a generic example of solitonic mesophase formation. This establishes the chiral magnetic ordering in noncentrosymmetric magnets as a new paradigm for unconventional phase transitions, which are expected to occur similarly in other systems described by the theory of incommensurate phases [3].

The ac susceptibility, χ_{ac}, of single crystalline ϵ-FeGe grown by chemical vapor transport [30] was measured in a Quantum Design PPMS device using a drive coil frequency of 1 kHz and an excitation field of 10 Oe. The well characterized single crystal ($m = 0.995$ mg) with almost spherical shape was aligned with the [100] axis parallel to the external magnetic field. Field sweeps were recorded such that the measuring T was always approached from 300 K in zero field and data were recorded upon increasing field. For T runs the sample was zero-field cooled.

Figure 1 shows $\chi_{ac}(H)$ for T in the vicinity of T_C. After an initial increase of $\chi_{ac}(H)$ a minimum starts to evolve at low H and for T in the range $272.5\ \text{K} < T < 279$ K. This dip in $\chi_{ac}(H)$ is well pronounced at 277 K and ceases as T approaches 273 K [Fig. 1(a)]. Lower and upper fields, H_A^1, H_A^2, delimiting the A region were extracted from the inflection points on either side of the minimum. Close to these fields maxima in the imaginary part, $\chi''_{ac}(H)$, were observed. Although a shallow minimum is found in $\chi_{ac}(H)$ at 278.5 K [see Fig. 1(b)] no maximum in $\chi''_{ac}(H)$ occurred.

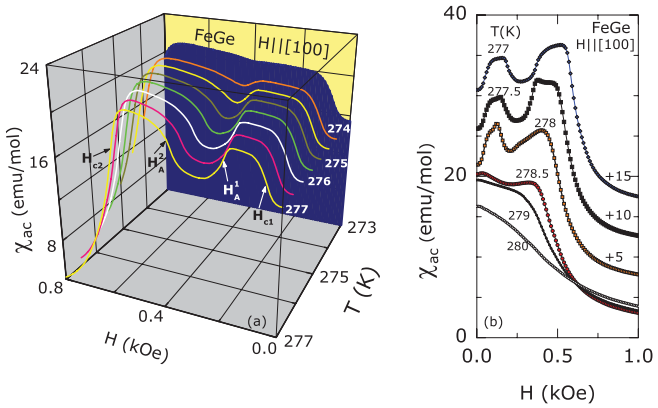

FIG. 1 (color). Isothermal $\chi_{ac}(H) = \sqrt{\chi'^2 + \chi''^2}$ data of ϵ-FeGe for $H \parallel [100]$. (a) The evolution of a well-defined minimum in $\chi_{ac}(H)$ upon approaching T_C from low T is the fingerprint of the A region. (b) Very close to T_C subtle changes in $\chi_{ac}(H)$ below about 0.6 kOe indicate a complex sequence of magnetic phase transitions and crossovers.

Further inflection points below and above at A region were used to define the critical fields H_{c1} and H_{c2}, corresponding to the entrance into the cone structure, and the spin-flip into the field-polarized (FP) state, respectively. Near H_{c1} also a peak in $\chi''_{ac}(H)$ was found. Cycling H at 276 K reveals a hysteresis of the order of 20 Oe near all transition fields whereas only a small hysteresis with width below 10 Oe was observed near H_{c1} and H_{c2} at 275 K.

The A region also appears as a minimum in $\chi_{ac}(T)$ as depicted in Fig. 2(a). Again, defining the limits of this region by inflection points, two transition lines $T_A^L < T_A^H$ were deduced. In this H range we also find a peak in $\chi''_{ac}(T)$ [see inset to Fig. 2(b)]. It suggests that T_A^L and T_A^H mark a

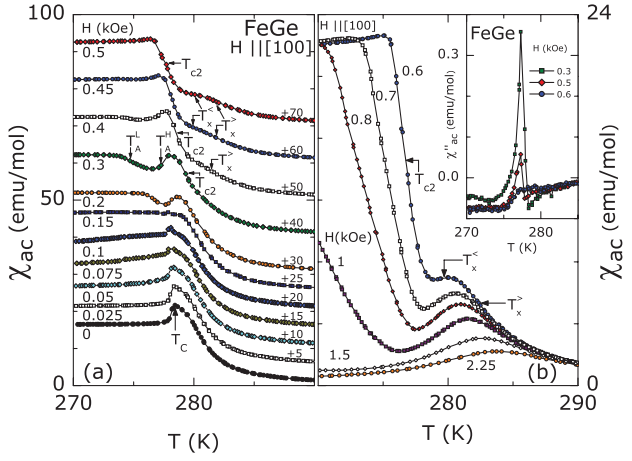

FIG. 2 (color). $\chi_{ac}(T)$ of ϵ-FeGe for constant $H \parallel [100]$. (a) The maximum at low H coincides with T_C. The shallow minimum for $H \geq 0.2$ kOe and $T_A^L < T < T_A^H$ is a signature of the A region. Curves are shifted vertically. (b) A broad maximum develops for $T_x^< < T < T_x^>$ and $H > 0.5$ kOe, indicating the crossover from the PM to the FP state. Inset: $\chi''_{ac}(T)$ shows a clear peak for $H \leq 0.5$ kOe related to the A region.

possibly discontinuous phase transition. Importantly, these transition lines extend towards higher H than the transition line H_A^2 found from field runs.

The shoulder in $\chi_{ac}(T)$ at about 280 K and for $H \gtrsim 0.45$ kOe [Fig. 2(a)] evolves into a clear maximum for $H > 0.6$ kOe [Fig. 2(b)] which broadens and shifts to higher T as H increases. Inflection points below and above this maximum at $T_\times^<$ and $T_\times^>$ signal a smeared crossover from the PM into the FP state at fields $H_\times^<$ and $H_\times^>$, respectively. Related to this feature is a very shallow minimum in $\chi''_{ac}(T)$ between $T_\times^<$ and $T_\times^>$. $H_\times^>(T)$ extrapolates to zero at $T_0 \simeq 280$ K. This implies that an intermediate state exists between T_0 and T_C which, depending on H, transforms into different magnetically ordered states at lower T. These transitions are visible in the $\chi_{ac}(T)$ data [Fig. 2(a)]. The transition into the helical state is seen as a cusp close to T_C for $0 < H < 50$ Oe, while the transition into the conical helix is seen as a tiny peak (data for $H = 0.1$ kOe). For $H > 0.1$ kOe, the entrance into the A region is observed by a markedly changed behavior of $\chi_{ac}(T)$.

More details of the magnetic properties in this T range are provided by $\chi_{ac}(H)$ depicted in Fig. 1(b). Clearly, the overall H dependence of $\chi_{ac}(H)$ changes strongly in the narrow T range $277.5\ \text{K} \leq T \leq 279$ K and for $H \lesssim 0.5$ kOe. The characteristic anomalies present up to 278 K appear completely smeared at 278.5 K where only a shallow minimum is visible between 0.1 and 0.28 kOe. Just a smooth decrease of $\chi_{ac}(H)$ remains for $T \geq 279$ K which indicates a crossover towards the FP state. Correspondingly, in $\chi_{ac}(T)$ a similar crossover is seen for $0.2\ \text{kOe} < H < 0.35$ kOe and in the same T range $279\ \text{K} < T < 280$ K [Fig. 2(a)].

This information is summarized in the phase diagram presented in Fig. 3. Long-range magnetic order sets in at $T_C = 278.2(3)$ K (for $H = 0$). The helical modulation along the [100] direction persists below H_{c1} which is of the order of 60 Oe. For larger external H the propagation direction is forced into the direction along H and a conical helix is formed. Finally, the fully FP state is entered at the spin-flip field H_{c2} where the cone angle closes. This is the normal behavior of a cubic helimagnet which is observed in the major T range below T_C [14,26]. However, the A region observed between about 273 and 278 K is found to be split into several distinct pockets. The main part, designated A_1 in Fig. 3, is clearly separated by a phase transition from phase A_2 which exists at higher fields. The magnetic structure of the A_2 region, however, appears to transform continuously into the conical phase, as $\chi_{ac}(T)$ for increasing H does not show clear anomalies above 0.5 kOe. There are two other small pockets A_0 and A_3 which are distinct from A_1 and the conical phase.

The FP state is separated from the PM phase by a broad crossover region (lines labeled as $H_\times^<$ and $H_\times^>$ in Fig. 3). This transforms below about 0.45 kOe into a region with precursor states between T_C and T_0 (straight dashed lines),

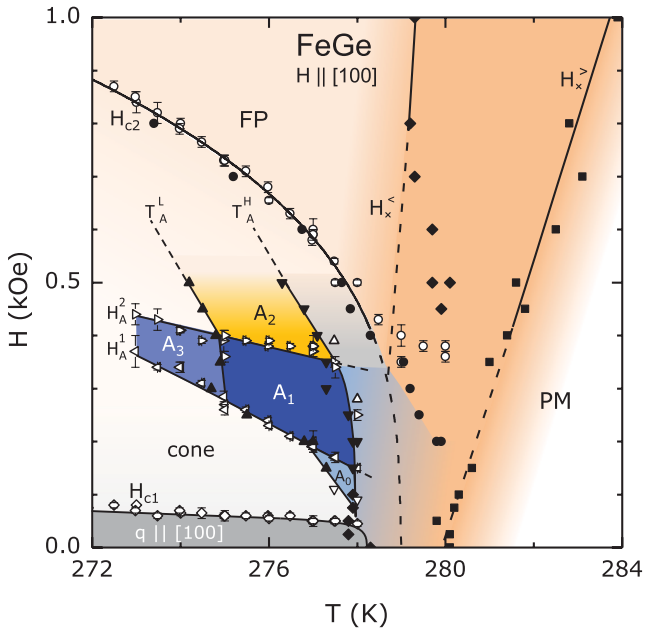

FIG. 3 (color). (H, T)-phase diagram of ϵ-FeGe for $H \parallel [100]$. Open and bold symbols represent data obtained from $\chi_{ac}(H)$ and $\chi_{ac}(T)$, respectively. Various phases are observed below $T_C = 278.2$ K: a helical state with $q \parallel [100]$ $(H < H_{c1})$, a conical helix phase (cone), a field-polarized state (FP) above H_{c2}, and a complex A region with several pockets. Various crossovers occur in the range $T_C < T < T_0 \simeq 280$ K and $H \lesssim 0.45$ kOe. The lines $H_x^<(T)$ and $H_x^>(T)$ indicate a crossover from the paramagnetic phase (PM) to the FP state. The dashed lines are high-field extrapolations.

inferred from smeared anomalies in H and T runs. Moreover, closer to the A region there is evidence of further transformations or crossovers that could not be resolved, e.g., related to the shallow anomaly in $\chi_{ac}(H)$ at 278.5 K [Fig. 1(b)].

The theoretical analysis of these findings is based on a phenomenological model [3,4]

$$w = A(\mathbf{grad}\mathbf{M})^2 - D\mathbf{M} \cdot \mathrm{rot}\mathbf{M} - \mathbf{H} \cdot \mathbf{M} + w_0(M) \quad (1)$$

with $w_0(M) = \alpha(T_C^0 + \Delta_D/4 - T)M^2 + bM^4$, where T_C^0 is the ferromagnetic Curie temperature and $\Delta_D = D^2/(2\alpha A) \ll T_C^0$ is the exchange shift, which increases the magnetic transition to T_N or T_S for helices or Skyrmions, respectively; A is the exchange stiffness and D is the DM interaction. Model (1) is commonly used to study precursor effects in cubic helimagnets [2,13,17,20].

Minimization of functional (1) shows [19] that in the magnetic phase diagram different types of chiral modulations are separated by a crossover line

$$H = H_0\sqrt{(1 \pm \nu)}\left(\frac{1}{2} \pm \nu\right)^2, \qquad T = T_{cf} + \Delta_D\nu^2, \quad (2)$$

with running parameter ν. $T_{cf} = T_C^0 - \Delta_D$ is the confinement temperature and $H_0 = \Delta_D\sqrt{2\Delta_D/b}$.

The solutions of (1) for $T < T_{cf}$ consist of helical or Skyrmionic textures with localized repulsive cores. They are essentially similar to solutions derived earlier for model (1) with a fixed magnetization modulus [3,18,22]. Near the ordering T, however, the interaction potential between helical kinks or Skyrmions is attractive. The crossover from repulsive to attractive is caused by the "softening" of the magnetization near the magnetic ordering. This imposes a coupling between angular (twisting) and longitudinal modulations of the magnetization magnitude [19,31,32]. As a result, chiral modulations in the confinement region, $T > T_{cf}$, drastically differ from regular repulsive modulations, because the magnetization modulus becomes inhomogeneous. The intercore coupling acquires an oscillatory and competing character. Thus, the magnetic properties are determined by an inherent frustration. Localized (particlelike) chiral modulations with oscillatory interactions can be arranged into various extended spin textures with tiny energy barriers. This confinement of localized states is a generic property of model (1). At the magnetic ordering itself, the attractive interactions cause a simultaneous nucleation and condensation of stable solitonic units into different clusters or extended bound configurations (mesophases). Rigorous solutions for the two-dimensional model (1) are sketched in Fig. 4; they can be homogeneously extended into the third space dimension as space-filling textures. The H-driven transformation of such modulated states evolves by distortions of the longitudinal components of the magnetization modulus while the equilibrium periods hardly change with H.

The characteristic features of attracting modulations, i.e., inherent frustration of clustered solitonic states and inhomogeneity of the order parameter both in directional and longitudinal components, show why various anomalous precursor states arise in cubic helimagnets above T_{cf}. The heuristically introduced "precursor region" should be identified with the T interval $T_{cf} < T < T_S$. The existence of this T range explains the complexity of the experimental phase diagram in FeGe (Fig. 3) and the diversity of earlier observations on anomalous magnetic ordering processes in other chiral helimagnets [9–15,33]. Magnetic noncentrosymmetric systems ruled by model (1), thus, are characterized by an unusual type of magnetic ordering relying on confined solitonic units.

The competition of extended spin textures in realistic chiral magnetic systems then is governed by additional magnetic energy contributions such as, e.g., anisotropies, dipolar interactions, fluctuations, etc., No clear hierarchy between these magnetic interactions is possible in the confinement region, in contrast to the simpler behavior at lower T. However, some characteristic features of the phase diagram (Fig. 3) can be interpreted in the framework of the modified Dzyaloshinskii model [20] $(\mathbf{grad}\mathbf{M})^2 \rightarrow M^2\sum_{i,j}(\partial_i n_j)^2 + \eta\sum_i(\partial_i M)^2$. The parameter η is unity for a "Heisenberg" model; i.e., the longitudinal stiffness of

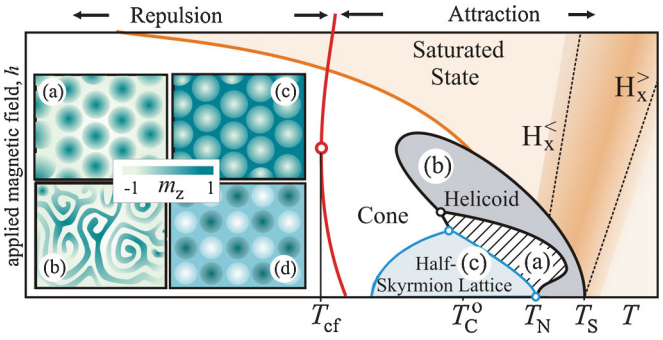

FIG. 4 (color). A densely packed full $+\pi$ Skyrmion lattice is found in region (a). The helicoid transverse to H is reentrant in region (b). Region (c) is a half-Skyrmion lattice with defects. Insets are maps of the magnetization component m_z for the different modulated magnetic structures in cutting planes perpendicular to H along $\mathbf{z}$. (a) $+\pi$ Skyrmion lattice; (b) spiral-domain texture of helicoids, adapted from pictures of cholesterics with polygonalized helix domains [34]; (c) half-Skyrmion square lattice; (d) $-\pi$-Skyrmion lattice for $T \ll T_{cf}$.

the pseudomicroscopic underlying theory is infinite. Confined chiral modulations are sensitive to values $\eta < 1$.

The magnetic phase diagram calculated for $\eta = 0.8$ includes pockets with square half-Skyrmion lattices, a hexagonal Skyrmion lattice with the magnetization in the center of the cells parallel to H, and helicoids with propagation transverse to H. The hexagonal $+\pi$-Skyrmion lattice [label (a) in Fig. 4] indicates the existence of densely packed phases of Skyrmion strings [18,19]. This Skyrmion phase competes with a helicoidal phase (b) stabilized at higher H. In contrast, the $-\pi$-Skyrmion lattice states expected to form a metastable low-T phase in chiral cubic helimagnets [21,22], do not exist near magnetic ordering in this model. At low H, a half-Skyrmion lattice (c) suggests a further competing type of precursor with split Skyrmionic units and defect points or lines, where magnetization passes through zero. At lower T, long-range ordered condensed phases may finally form. The observed T_C is expected below T_N owing to the competition with spontaneous half-Skyrmion states [20].

A comparison of the experimental phase diagram with the theoretical results suggests to identify the pocket A_1 with a densely packed phase consisting of full $+\pi$ Skyrmions, the region and inset (a) in Fig. 4. The pocket A_2 at higher H then should be a reentrant helicoidal state labeled as (b) in Fig. 4. A helicoid can be continuously transformed by reorientation of the propagation direction into the conical state. This conforms with the open region A_2 in Fig. 3. As we know the A_2 region to display characteristic sixfold Bragg patterns in our preliminary magnetic small-angle neutron scattering, this area most likely is a polygonalized helix-domain structure. Such defect textures are well known from cholesteric liquid crystals [34] that obey a similar phenomenological theory as chiral magnets. In these helicoidal textures, domains with nearly circular cross section containing spiralling helices are arranged into lattices or into a hexatic orientational order. Spiralling domains of the helicoidal spin-structure have earlier been seen in FeGe thin films [24].

In conclusion, the ac-magnetic susceptibility data on ϵ-FeGe show a complex sequence of phase transitions and crossovers in the vicinity of T_C. The A-phase region is not homogeneous, but split into several parts. The results exemplify the complex nature of precursor phenomena in cubic helimagnets with chiral DM couplings. The crossover of intersoliton coupling from repulsive to attractive in the confinement region, $T_{cf} < T < T_S$, provides the mechanism that explains the complex and anomalous magnetic ordering processes and the occurrence of various mesophases interleaved between paramagnetic and helical ground states in FeGe and other cubic helimagnets. This study shows that understanding spin-structures in the precursor region is incomplete and that the identification of Skyrmions and Skyrmion lattices close to magnetic ordering is an open problem.

We acknowledge discussions with Yu. Grin and technical assistance from R. Koban, Yu. Prots, and H. Rave and support by DFG project RO 2238/9-1.

[1] N. Manyala *et al.*, Nature (London), **454**, 976 (2008).
[2] X. Z. Yu *et al.*, Nature (London) **465**, 901 (2010).
[3] I. E. Dzyaloshinskii, Sov. Phys. JETP **19**, 960 (1964).
[4] P. Bak and M. H. Jensen, J. Phys. C **13**, L881 (1980).
[5] S. Kusaka *et al.*, Solid State Commun. **20**, 925 (1976).
[6] T. Komatsubara *et al.*, in *Proceedings 6th Intern. Conf. Internal Friction and Ultrasonic Attenuation in Solids* (University of Tokyo Press, Tokyo, 1977) p. 237.
[7] C. Thessieu *et al.*, J. Phys. Condens. Matter **9**, 6677 (1997).
[8] A. Neubauer *et al.*, Phys. Rev. Lett. **102**, 186602 (2009).
[9] K. Kadowaki *et al.*, J. Phys. Soc. Jpn. **51**, 2433 (1982).
[10] Y. Ishikawa and M. Arai, J. Phys. Soc. Jpn. **53**, 2726 (1984).
[11] C. I. Gregory *et al.*, J. Magn. Magn. Mater. **104-107**, 689 (1992).
[12] D. Lamago *et al.*, Physica (Amsterdam) **385-386B**, 385 (2006).
[13] S. Mühlbauer *et al.*, Science **323**, 915 (2009).
[14] B. Lebech *et al.*, J. Magn. Magn. Mater. **140–144**, 119 (1995).
[15] S. V. Grigoriev *et al.*, Phys. Rev. B **73**, 224440 (2006).
[16] S. V. Grigoriev *et al.*, Phys. Rev. B **74**, 214414 (2006).
[17] S. V. Maleyev, arXiv:1102.3524.
[18] U. K. Rößler *et al.*, J. Phys. Conf. Ser. **303**, 012105 (2011).
[19] A. A. Leonov *et al.*, arXiv:1001.1292v3.
[20] U. K. Rößler *et al.*, Nature (London) **442**, 797 (2006).
[21] A. N. Bogdanov and D. A. Yablonskii, Sov. Phys. JETP **68**, 101 (1989).
[22] A. N. Bogdanov and A. Hubert, J. Magn. Magn. Mater. **138**, 255 (1994).
[23] M. Uchida *et al.*, Science **311**, 359 (2006).
[24] M. Uchida *et al.*, Phys. Rev. B **77**, 184402 (2008).

[25] X. Z. Yu *et al.*, Nature Mater. **10**, 106 (2011).
[26] B. Lebech *et al.*, J. Phys. Condens. Matter **1**, 6105 (1989).
[27] L. Lundgren *et al.*, Phys. Scr. **1**, 69 (1970).
[28] P. Pedrazzini *et al.*, Phys. Rev. Lett. **98**, 047204 (2007).
[29] L. Lundgren *et al.*, Phys. Lett. A **28**, 175 (1968).
[30] H. Wilhelm *et al.*, Sci. Tech. Adv. Mater. **8**, 416 (2007).
[31] B. Schaub and D. Mukamel, Phys. Rev. B **32**, 6385 (1985).
[32] M. Yamashita and O. Tamada, J. Phys. Soc. Jpn. **54**, 2963 (1985).
[33] C. Pappas *et al.*, Phys. Rev. Lett. **102**, 197202 (2009).
[34] Y. Bouligand, Tissue and cell **4**, 189 (1972).